

Magma Interaction Recorded in Plagioclase Zoning in Granitoid Systems, Zigana Granitoid, Eastern Pontides, Turkey

ORHAN KARSLI¹, FARUK AYDIN² & M. BURHAN SADIKLAR³

¹ Department of Geological Engineering, Karadeniz Technical University, TR-29000 Gümüşhane – Turkey
(e-mail: okarsli@ktu.edu.tr)

² Department of Geological Engineering, Niğde University, TR-51200 Niğde – Turkey

³ Department of Geological Engineering, Karadeniz Technical University, TR-61080 Trabzon – Turkey

Abstract: Plagioclase crystals characterized by compositional zoning are typical of the Zigana Granitoid (ZG), NE Turkey. The zoned crystals, which show textural equilibrium with the assemblage quartz + plagioclase + K-feldspar + hornblende + biotite + pyroxene + magnetite + ilmenite, exhibit oscillatory zoning. The zoned plagioclase crystals, ranging in size from 3 to 6 mm, are oval and larger than normal lath-shaped crystals. The zoned crystals are divided petrographically into two main types: (i) crystals zones only at their rims, with spongy cores; and (ii) completely zoned ones. Composition of the zoned crystals ranges from An₂₃ (oligoclase) to An₇₀ (labradorite). Plagioclase crystals with oscillatory zoning are governed by strong substitution mechanisms of Ca²⁺ ⇌ Na⁺, Al³⁺ ⇌ Si⁴⁺ and weak substitution of Fe³⁺ for Si⁴⁺. The Fe₂O₃^(t) (wt %) contents of the subject plagioclases increase with increasing An content. The petrographic and compositional changes from rim to rim (oscillatory zoning), and positive correlation between Fe₂O₃^(t) (wt %) and An (mol %) contents of the zoned plagioclases, suggest recurrent mafic magma injection into a felsic magma chamber, and thus magma interaction as a dominant magmatic process during the evolution of the Zigana Granitoid (ZG).

Key Words: plagioclase, oscillatory zoning, mafic-felsic magma interaction, Zigana Granitoid, eastern Pontides, Turkey

Granitoyidik Sistemlerdeki Plajiyoklaz Zonlanmasında Kayıt Edilen Magma Etkileşim İzleri, Zigana Granitoyidi, Doğu Pontidler, Türkiye

Özet: Bileşimsel zonlanma ile karakterize olan plajiyoklaz kristalleri Zigana Granitoyidi'nde (ZG), KD-Türkiye tipik olarak gözlenmektedir. Kuvars + plajiyoklaz + K-feldspat + hornblend + biyotit + piroksen + magnetit + ilmenit denge kristaleşmesi sunan zonlu plajiyoklaz kristalleri salınımlı (oscillatory) zonlanma gösterirler. Kristal boyları 3 ile 6 mm arasında değişen zonlu plajiyoklaz kristalleri çoklukla oval biçimli olup, normal lata biçimlilerden daha büyütüktürler. Zonlu plajiyoklazlar petrografik olarak, tamamen zonlu ve merkezi süngerimsi kenarı zonlu kristaller olmak üzere iki ana grupta toplanmışlardır. Zonlu kristallerin bileşimleri An₂₃ (oligoklaz) ile An₇₀ (labradorit) arasındadır. Salınımlı zonlu plajiyoklaz kristalleri kuvvetli Ca²⁺ ⇌ Na⁺, Al³⁺ ⇌ Si⁴⁺ ve zayıf Fe³⁺ ⇌ Si⁴⁺ sübsitusyon mekanizması ile kontrol edilirler. Plajiyoklazların Fe₂O₃^{top} (% ağ.) konsantrasyonu, An içeriği ile artısunar. Zonlu kristallerin petrografik, kenardan kenara kimyasal değişimleri ve mol % An içerikleri ile Fe₂O₃^{top} konsantrasyonları arasındaki pozitif ilişki, Zigana Granitoyidi nin (ZG) oluşumu sırasında felsik magma odasına sürekli bir mafik injeksiyonun varlığına ve dolayısıyla magma etkileşiminin ağırlıklı magmatik olay olabileceğini yansıtmaktadır.

Anahtar Sözcükler: plajiyoklaz, salınımlı zonlanma, mafik-felsik magma etkileşimi, Zigana Granitoyidi, doğu Pontidler, Türkiye

Introduction

Plagioclase crystals in magmatic rocks possess various textural types and zoning such as spongy, boxy and sieve texture, and oscillatory, patchy and normal zoning. These textures provide us with information concerning

conditions of magmatic evolution and histories of magmatic systems. Spongy and boxy textures are attributed to magma interaction and assimilation processes (e.g., Lofgren & Donaldson 1975; Hibbard 1991; Castro 2001). Sieve textures in plagioclase indicate

rapid decompression (Stomer 1972; Kuşçu-Gençalioğlu & Floyd 2001) and magma mixing (Wiebe 1968; Pringle *et al.* 1974; McDowell 1978; Nelson & Montana 1992; Tsuchiyama 1985) in magma chambers, while oscillatory zoning infers repeated injections of mafic melts, fluctuations in total pressure or temperature, changes in a_{H_2O} of magmas, or diffusion-crystallization kinetics (Hattori & Sato 1996). In addition, patchy zoning is interpreted to be caused by rapid increase in crystals, decompression, supersaturation, and/or decrease in confining pressure on water-deficient magma during crustal ascent (Vance 1962, 1965; Anderson 1984). Recently, Tegner (1997) studied iron changes in magmatic plagioclase to elucidate magma differentiation records in the Skaergaard intrusion.

In choosing the reverse-zoned Zigana Granitoid (ZG) due to its well-known geochemical character and tectonic setting, and its similarity to the other intrusions in the same magmatic belt, we aim to determine magmatic conditions and magmatic history of granitoid rocks in the Pontide Belt by explaining the morphologies and chemical characters of zoned plagioclase crystals in the ZG. Accordingly, we have investigated plagioclase compositions, plagioclase zoning models, the effects of magma interaction or re-injection, and the differentiation stages of the pluton.

Geological Setting of the Zigana Granitoid

The Zigana Granitoid, situated in the northern zone of the eastern Pontides (EP), lies in a N–S line across the 500-km-long section (Ketin 1966; Bektaş 1986; Bektaş *et al.* 1995) (Figure 1). The EP comprises: (1) Devonian metamorphic rocks, (2) Lower Carboniferous granitoid and dacitic rocks, (3) Upper Carboniferous–Lower Permian shallow-marine to terrigenous sedimentary rocks, (4) Permo-Triassic metabasalt–phyllite–marble, (5) a 200-m-thick sequence of Lower and Middle Jurassic tuff, pyroclastic rocks, lavas and interbedded clastic sedimentary rocks, (6) Upper Jurassic–Lower Cretaceous carbonates, (7) Lower Cretaceous ophiolitic mélange, (8) Middle–Upper Cretaceous to Middle Eocene granitoid plutons and volcanic rocks ranging in composition from basalt and andesite to dacite, (9) Upper Palaeocene–Lower Eocene major foreland flysch, and post Eocene terrigenous units (e.g., Ketin 1966; Çoğulu 1975; Taner 1977; Şengör & Yılmaz 1981; Keskin *et al.*

1989; Güven 1993; Okay 1993, 1996; Bektaş *et al.* 1995, 1999; S. Yılmaz & Boztuğ 1996; C. Yılmaz 1995, 1996, 1997, 2002; Okay & Şahintürk 1997; C. Yılmaz & Karslı 1997; Y. Yılmaz *et al.* 1997; Kandemir & Korkmaz 1999; Boztuğ *et al.* 2004a).

Many intrusive bodies have been described from the eastern Pontides. These bodies developed in various geodynamic settings, and have different ages and compositions. They range from Early–Late Cretaceous (Taner 1977; Moore *et al.* 1980; JICA 1986; Okay & Şahintürk 1997; Y. Yılmaz *et al.* 1997; Boztuğ *et al.* 2001, 2004a, b; Karslı *et al.* 2004a) to Eocene (S. Yılmaz & Boztuğ 1996; Boztuğ 2001; Boztuğ *et al.* 2001; Karslı 2002; Karslı *et al.* 2002, 2004b) in age. In addition, their compositions vary from low-K tholeiitic through calc-alkaline (rarely high-K) metaluminous granitoids and peraluminous leucogranites to alkaline syenites and monzonites (S. Yılmaz & Boztuğ 1996; Boztuğ 2001; Boztuğ *et al.* 2001, 2004a, b; Karslı *et al.* 2002, 2004a); and from arc-collisional through syn-collisional crustal thickening to post-collisional extensional regimes (Yılmaz & Boztuğ 1996; Okay & Şahintürk 1997; Boztuğ 2001; Boztuğ *et al.* 2001; Karslı 2002; Karslı *et al.* 2002).

The ZG is a small part of the composite Kaçkar Batholith, dated 30 to 80 Ma (K/Ar on hornblende: Çoğulu 1975; Moore *et al.* 1980; JICA 1986 and fission-track on apatite: Boztuğ *et al.* 2004a), which lies along an E–W line in the northern zone of the eastern Pontides (Boztuğ *et al.* 2001, 2004a) (Figure 2). Furthermore, the age of the pluton is derived from stratigraphical relationships. The Early Eocene ZG intrudes Mesozoic to Cenozoic volcanic rocks, comprising andesite, basalt and their pyroclastic equivalents, in the study area (Karslı & Sadıkçılar 1996, 1997) (Figure 3), and was emplaced into a magmatic arc which was active from Late Cretaceous to Early Eocene (Şengör & Yılmaz 1981; Okay 1996; Okay & Şahintürk 1997; Yılmaz & Karslı 1997; Yılmaz *et al.* 1997; Bektaş *et al.* 1999; Kandemir & Korkmaz 1999; Yılmaz 2002; Şengör *et al.* 2003).

Field, Petrographical, Mineralogical and Geochemical Characteristics

The ZG is a reverse-zoned intrusion and is represented by a series of granitoid rocks, comprising medium-grained granite, granodiorite, quartz monzodiorite, and

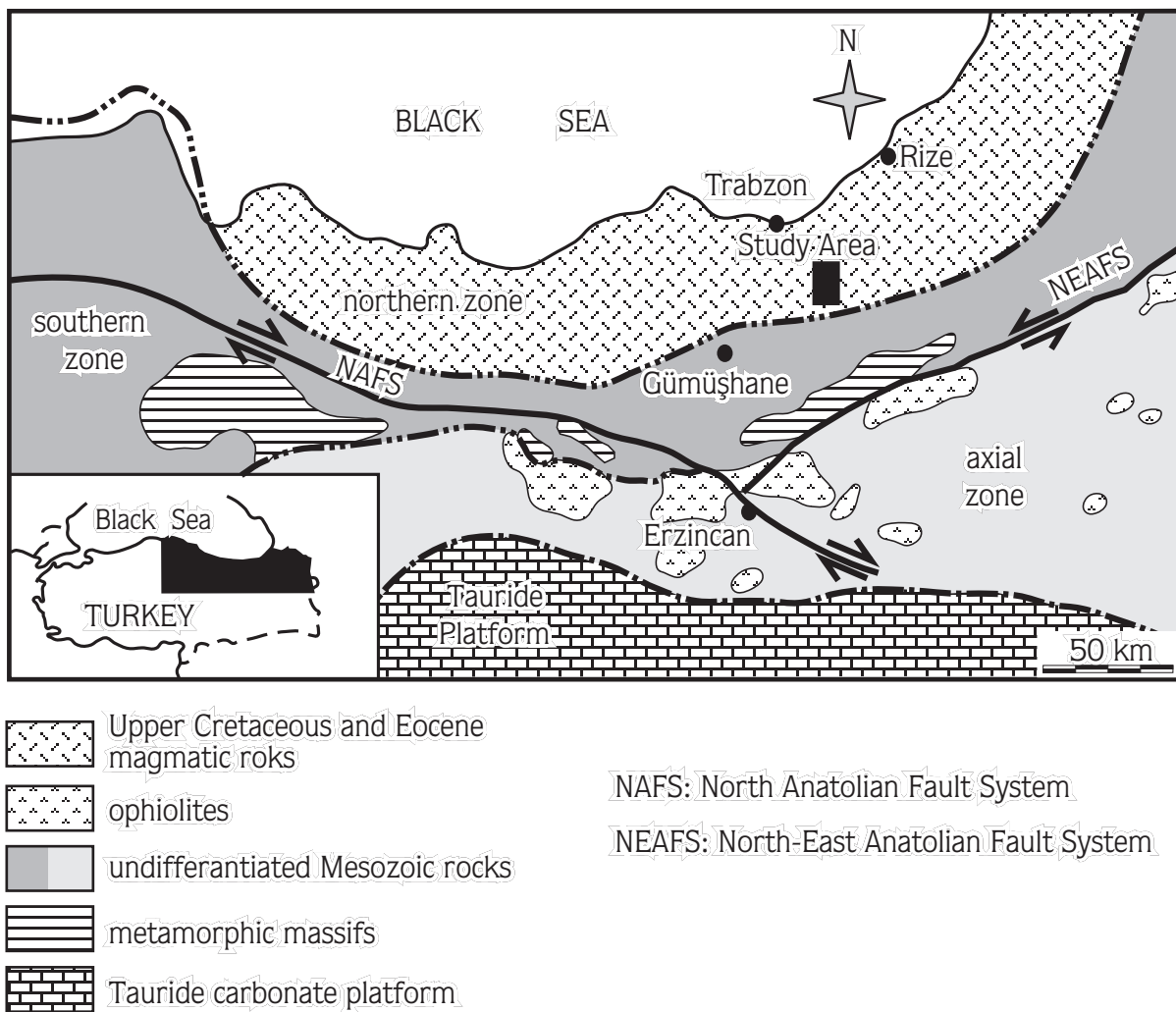


Figure 1. Location map of the study area and inferred boundary of the eastern Pontides (modified after Bektaş *et al.* 1995).

monzodiorite (Figure 3). Thus, the ZG has a more mafic composition at its core (monzodiorite), with more felsic (granite and granodiorite) outer zones. A quartz-monzodioritic zone is transitional in composition between the two zones (Karslı & Sadıkclar 1997) (Figure 3). Reverse- and normal-zoned plutonic bodies are widespread among the Cenozoic granitoid rocks formed within the calc-alkaline suite of the Pontide Belt (Karslı 2002; Karslı *et al.* 2002).

More mafic rocks, which comprise the core of the pluton, solidified from monzodioritic to quartz-monzodioritic magmas, whereas more felsic rocks (granite and granodiorite) occur at the margin of the

pluton; this compositional trend parallels the increase in the number of elliptical mafic microgranular enclaves (20 cm to 1 mm in size) whose modal mineralogy ranges from diorite to monzodiorite. These features have sharp contacts – without metamorphic minerals – with the host granitoid rocks. This field evidence may be an indication of mafic and felsic magma interaction.

The typical magmatic mineral assemblage of the ZG is plagioclase + K-feldspar + quartz + hornblende + biotite + pyroxene (abundant clinopyroxene, minor orthopyroxene) + magnetite + ilmenite, in order of decreasing abundance. Titanite and apatite occur as accessory minerals. Quartz, K-feldspar and plagioclase

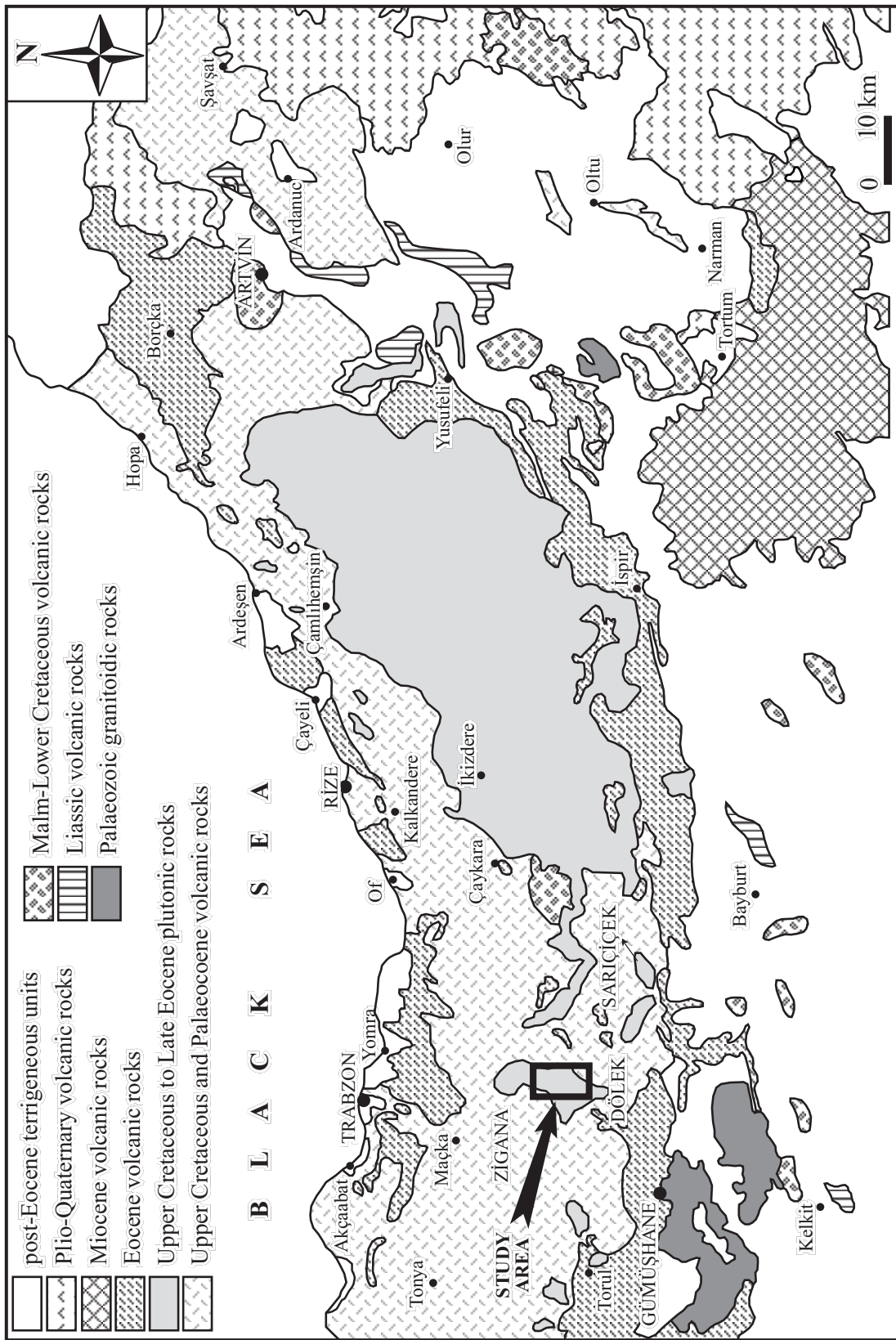


Figure 2. Simplified geological map of the eastern Pontides showing the distribution of granitoid plutons (modified after Gedik *et al.* 1992).

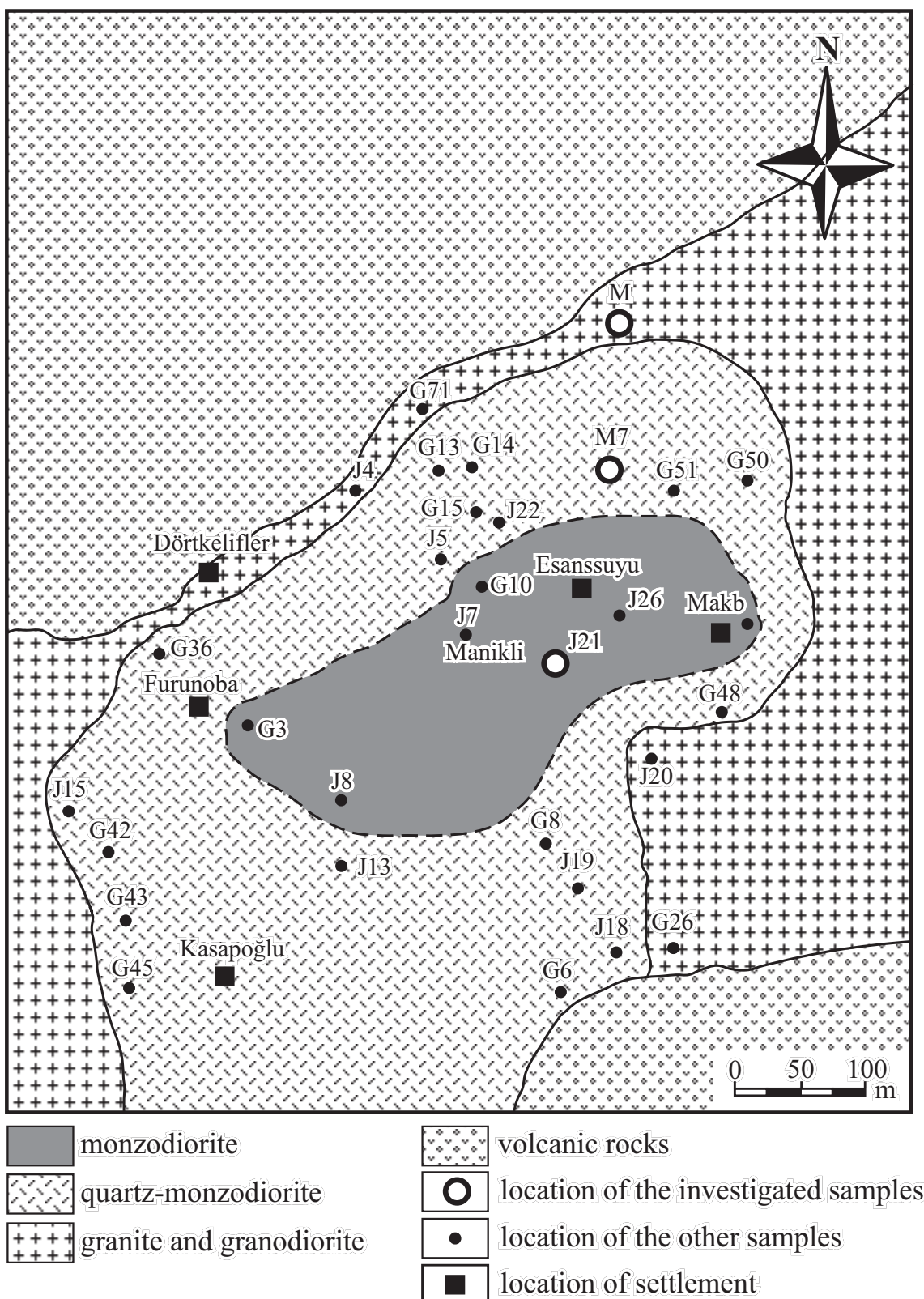


Figure 3. The geological and zonation map of the Zigana Granitoid (modified after Karsli & Sadıklar 1997).

contents are highly variable depending on rock types. Anhedral fragments of quartz are widespread. Subhedral orthoclase crystals ($\text{Or}_{97-85}\text{Ab}_{2-15}\text{An}_{1-0}$) always accompany other felsic and mafic minerals. All hornblendes of the pluton exhibit normal brownish-green pleochroism. Magnesio-hornblende with $\text{Mg}/(\text{Mg}+\text{Fe}^{2+})$ ratios ranging from 0.70 to 0.88 is observed as typically < 3 mm subhedral to euhedral crystals (4–7%). Hornblende crystals are in most cases smaller and more euhedral than biotites and clinopyroxenes ($\text{Di}_{75-71}\text{Hd}_{23-22}\text{En}_{2-7}$, augite; $\text{En}_{56}\text{Fs}_{32}\text{Wo}_{12}$, pigeonite) and orthopyroxenes ($\text{En}_{66}\text{Fs}_{32}\text{Wo}_2$, enstatite). Biotite crystals with $X_{\text{Mg}}=\text{Mg}/(\text{Mg}+\text{Fe}^{2+})$ ranging between 0.50 and 0.75 (4–9%) are observed as independent single crystals or as replacements of hornblende and pyroxene (6–10%) (Table 1). The hornblendes and biotites are partially altered to actinolite and chlorite, respectively. Magnetite

($\text{Mag}_{73-68}\text{Ulvö}_{27-32}$) and ilmenite ($\text{Ilm}_{98-67}\text{Hm}_{02-33}$) are generally primary phases. Some magnetites contain Ti-rich exsolution lamellae, and ilmenite is always associated with magnetite.

Textures characteristic of coeval felsic and mafic interaction, such as presence of blade biotite, exsolution-lamellae-bearing magnetite, elongate prismatic amphibole, acicular apatite and poikilitic plagioclase, quartz, K-feldspar, amphibole and biotite, are present in the ZG.

Samples Selection and Analytical Procedures

The samples used for analyses were collected from a traverse crossing the intrusion from the core through to the outer zone (Figure 3). The selected samples are

Table 1. Selected whole-rock chemical and modal compositions of rocks from the Zigana Granitoid.

Sample No	Zigana Granitoid monzodiorite containing hornblende, biotite and pyroxene		quartz monzodiorite containing hornblende, biotite and minor pyroxene			granodiorite to granite containing hornblende and minor biotite		
	J21	M7	J18	G36	J19	M5	G71	J4
CHEMICAL ANALYSES⁺								
SiO ₂	56.08	56.15	59.06	60.24	62.71	67.04	68.89	71.36
TiO ₂	0.53	0.56	0.39	0.45	0.36	0.33	0.32	0.30
Al ₂ O ₃	20.23	18.64	17.29	18.89	16.83	15.76	15.22	14.81
FeO ^t	5.89	5.70	2.44	5.32	3.99	3.03	3.01	3.19
MnO	0.08	0.05	0.03	0.07	0.06	0.03	0.05	0.07
MgO	4.29	3.13	1.44	3.16	2.03	1.06	1.02	1.11
CaO	6.00	6.52	7.59	4.22	5.54	3.44	3.30	2.17
Na ₂ O	2.06	4.21	5.05	3.73	4.38	4.11	3.55	3.60
K ₂ O	3.87	3.65	3.29	4.37	2.81	3.45	3.58	4.24
P ₂ O ₅	0.06	0.12	0.10	0.10	0.08	0.09	0.08	0.07
LOI	0.87	2.13	1.53	1.16	1.32	0.76	0.96	0.75
Total	99.9	100.8	98.2	100.7	100.1	99.1	99.9	101.8
MODAL ANALYSES								
Quartz	3	6	7	8	12	27	28	30
K-Feldspar	18	15	10	24	7	17	20	22
Plagioclase	58	70	73	56	70	51	45	40
Biotite	7	2	<1	2	3	<1	<1	1
Amphibole	6	4	5	3	5	4	5	6
Pyroxene	7	2	1	4	1	-	-	-
Mag.-Ilm.	1	1	4	3	2	1	2	1
Q (%)	4	7	8	9	13	28	30	33
A (%)	23	16	11	27	8	18	22	24
P (%)	73	77	81	64	79	54	48	43

+ Major oxide analyses were determined by ICP & XRF

t Toplam iron as FeO

representative of the three main zones of the intrusion, namely the outer zone [granite (Cr-M5) and granodiorite], the transitional zone [quartz monzodiorite (Cr-M7)] and inner zone [monzodiorite (Cr-J21)]. Compositions of the plagioclase crystals were determined using a CAMECA-SX-51 electron microprobe equipped with five wavelength-dispersive spectrometers in the Mineralogical Institute of Heidelberg University, Germany. Synthetic and natural oxides and silicates were used for calibration. The correction procedures were performed using CAMECA's PAP software. Operating conditions were 15 kV accelerating voltage and 20 nA beam current. 165 spot analyses were obtained in rim-to-rim traverses for each of three crystal types. Counting time was usually 10 s for major elements, i.e., Si, Al, Fe, Ca, Na and K. The analyses were performed with a beam diameter of 10 µm in order to minimize possible alkaline diffusion.

Whole-rock compositions were obtained via ICP spectrometry by ACME Laboratory, Canada, and in the geochemical laboratory of the Mineralogical Institute of Heidelberg University, by standard wavelength dispersive XRF techniques using lithium borate fusion disks and pressed powder pellets.

Whole-Rock Chemistry

In this study, a total of 40 fresh granitoid samples from the Zigana Granitoid were collected for analysis. Eight representative chemical analyses are given in Table 1.

The samples span a range of SiO₂ from about 56 to 72 wt %, namely granite, granodiorite, monzodiorite and quartz monzodiorite. The ZG rocks are assigned to the metaluminous and I-type granitoid categories because of their essential mineralogical and chemical properties (Karslı & Sadık 1996, 1997; Karslı *et al.* 2002). The aluminum saturation index [ASI = molecular Al₂O₃/(CaO+K₂O+Na₂O)] increases with SiO₂ from about 0.82 to 1.10 (Figure 5). Using the K₂O versus SiO₂ nomenclature of Peccerillo & Taylor (1976), the granitoid rocks are classified as high-K calc-alkaline rocks (Figure 5). Major elements versus SiO₂ plots (Harker diagrams) for granitoid rocks of the ZG suggest that fractional crystallization (FC) and/or crystal fractionation played important roles in the genesis of the granitoid rocks. Despite some scatter, these granitoid rocks display linear trends without compositional gaps in most plots (Figure

6), suggesting that, in addition to the FC process, magma mixing may also have been important in the evolution of the granitoid rocks. Magma mixing is also supported by the linear trends for all major elements, and by textural relationships and chemical properties of characteristic minerals, to be discussed below.

The granitoids developed in different tectonic environments with different ages and chemical compositions and, as mentioned above, represent different petrologic processes. These Cretaceous and Early Cenozoic arc-related granitoids, with calc-alkaline (sometimes high-K calc-alkaline), metaluminous and I-type compositions, possess well-preserved evidence of magma interactions between coeval mafic and felsic magmas (Karslı 1996; S. Yılmaz & Boztuğ 1996; Okay & Şahintürk 1997; Boztuğ 2001; Boztuğ *et al.* 2001, 2004b; Karslı 2002; Karslı *et al.* 2004a, b). This plutonic unit was called the first plutonic phase south of the Giresun area in the northern zone of the eastern Pontides by Yılmaz & Boztuğ (1996). The mineralogical and whole-rock chemical characteristics of the ZG resemble those of the first plutonic phase. The plutonic phase, comprising the ZG, is explained as a part of the well-known south-facing Pontide magmatic arc of Albian to Oligocene age, induced by northward subduction of the northern branch of Neotethys beneath the Eurasian plate (Şengör & Yılmaz 1981; S. Yılmaz & Boztuğ 1996; Okay 1996; Y. Yılmaz *et al.* 1997; Şengör *et al.* 2003). The ZG has also been interpreted as a volcanic arc granitoid (VAG) on the basis of its trace-element concentrations (Karslı 1996; Karslı & Sadık 1996).

Morphology and Composition of Plagioclase

Plagioclase, the most abundant mineral in the ZG, occurs mainly with three different types of morphology, namely, oscillatory zoned crystals (completely zoned crystals – P1) (Figure 4a), spongy-cellular cores with zoned rims (P2) (Figure 4b, c), and lath-shaped crystals (P3) (Figure 4b). Representative chemical analyses of all plagioclase crystal types of the ZG are presented in Table 1. The lath-shaped unzoned crystals (P3) are ~1–3 mm in length and have compositions of An_{40–45} (andesine) (Figure 7d). The P1 and P2 crystal types, which are generally ~1–6 mm in size and oval in shape, were chosen for detailed investigation.

An contents (mol %) of the zoned crystals (P1 and P2) vary from 35 to 70, but are mostly between 45 and

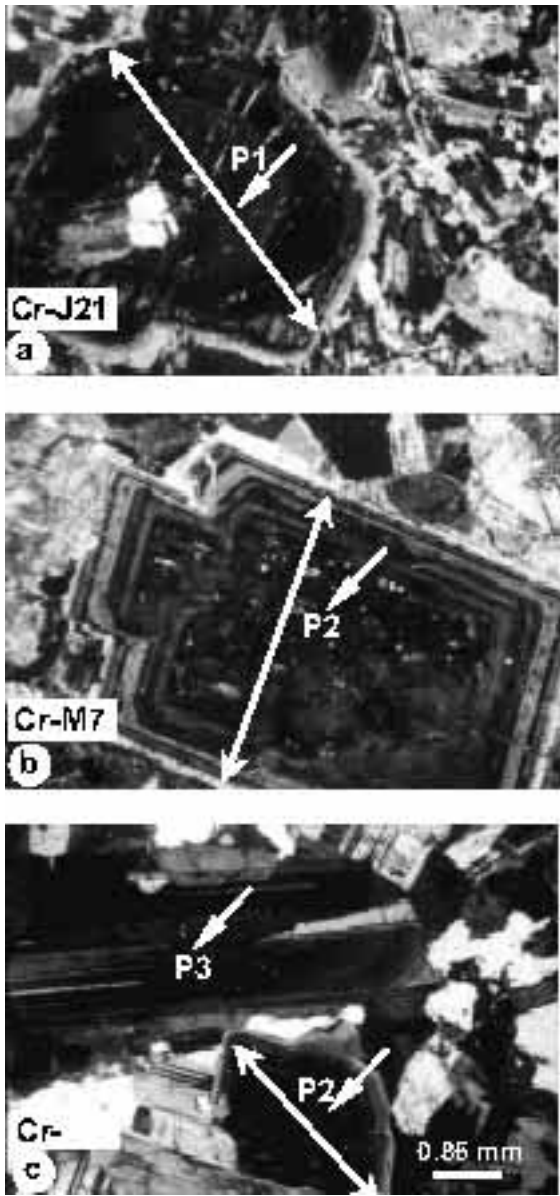


Figure 4. Photomicrographs showing typical textures of plagioclase crystals from the Zigana Granitoid. Position of profiles in Figure 7 is shown in a, b and c.

55 (Figures 5, 6 & 7). The K_2O (wt %) content varies from 0.12 to 0.70. The average of SiO_2 (wt %) and Al_2O_3 (wt %) contents of the zoned plagioclases (P1 and P2) are 53.9 and 29.0, respectively (Table 2). Completely zoned plagioclase crystals (P1) show oscillatory zoning with compositions of An_{70} to An_{34} (labradorite to oligoclase) from rim to rim (Figures 7a & 8a). The crystals with spongy-cellular cores and zoned rims, have ~ 45–53 mol % An cores.

The zoned plagioclase compositions are defined by the substitution mechanisms $Ca^{2+} \leftrightarrow Na^+$, $Al^{3+} \leftrightarrow Si^{4+}$ and $Fe^{3+} \leftrightarrow Si^{4+}$; the $Fe^{3+} \leftrightarrow Si^{4+}$ substitution is weaker than the first two mechanisms (Figure 9a–c). The $Fe_2O_3^{(t)}$ (wt %) contents vary between 0.1 and 0.88 and increase from the outer zone to the inner zone of the ZG. Moreover, this chemical characteristic positively correlates with An content (mol %) (Figure 9d).

Significance of Plagioclase Zoning

Various non-linear models have been proposed to explain the origin of zoning in plagioclase. The zoning of plagioclase is controlled by its An (mol %) variation (Yoder *et al.* 1957; L'Heureux & Fowler 1994; Hattori & Sato 1996). Changes in An content of igneous plagioclase crystals may be caused by diffusion-crystallization kinetics when: (a) diffusion of Al^{3+} for Si^{4+} and Ca^{2+} for Na^+ in melt occurs (L'Heureux & Fowler 1994), and (b) recurrent injection of mafic magma resulting in An spikes in igneous plagioclase crystal is observed (Luhr & Melson 1996). Complex zoning patterns are preserved in plagioclase owing to the coupling substitutions mentioned above. These complex zoning patterns record complex crystal morphologies produced as the crystals grew from a silicate melt (L'Heureux & Fowler 1994). In addition, the An content of plagioclase is governed by total temperature and pressure (Hattori & Sato 1996), An content of the parent magma, and H_2O content of magma (Johannes 1978; Housh & Luhr 1991). All of these factors may result in compositional-gradient oscillatory zoning.

Oscillatory zoning is a widespread feature in plagioclases of the monzodioritic core of the ZG where plagioclase compositions range between An_{34} and An_{70} . Oscillation patterns ranging from 5 to 40 μm in width have An_{10-30} variations in plagioclase of the inner zone of the intrusion. The oscillation ranges from 5 to 60 μm in width and An_{5-25} plagioclase in the outer zone of the intrusion (Figure 8). The widths and amplitudes of variations are higher in the rims of the crystals than in the cores. Amplitudes of oscillation are lower in plagioclase of the outer zone than those of plagioclases in the inner zone. The P2-type plagioclase morphology may result from destabilization of the crystal-melt interface caused by the disequilibrium production of a Ca-rich mafic melt (Castro 2001). The occurrence of Ca-rich metastable

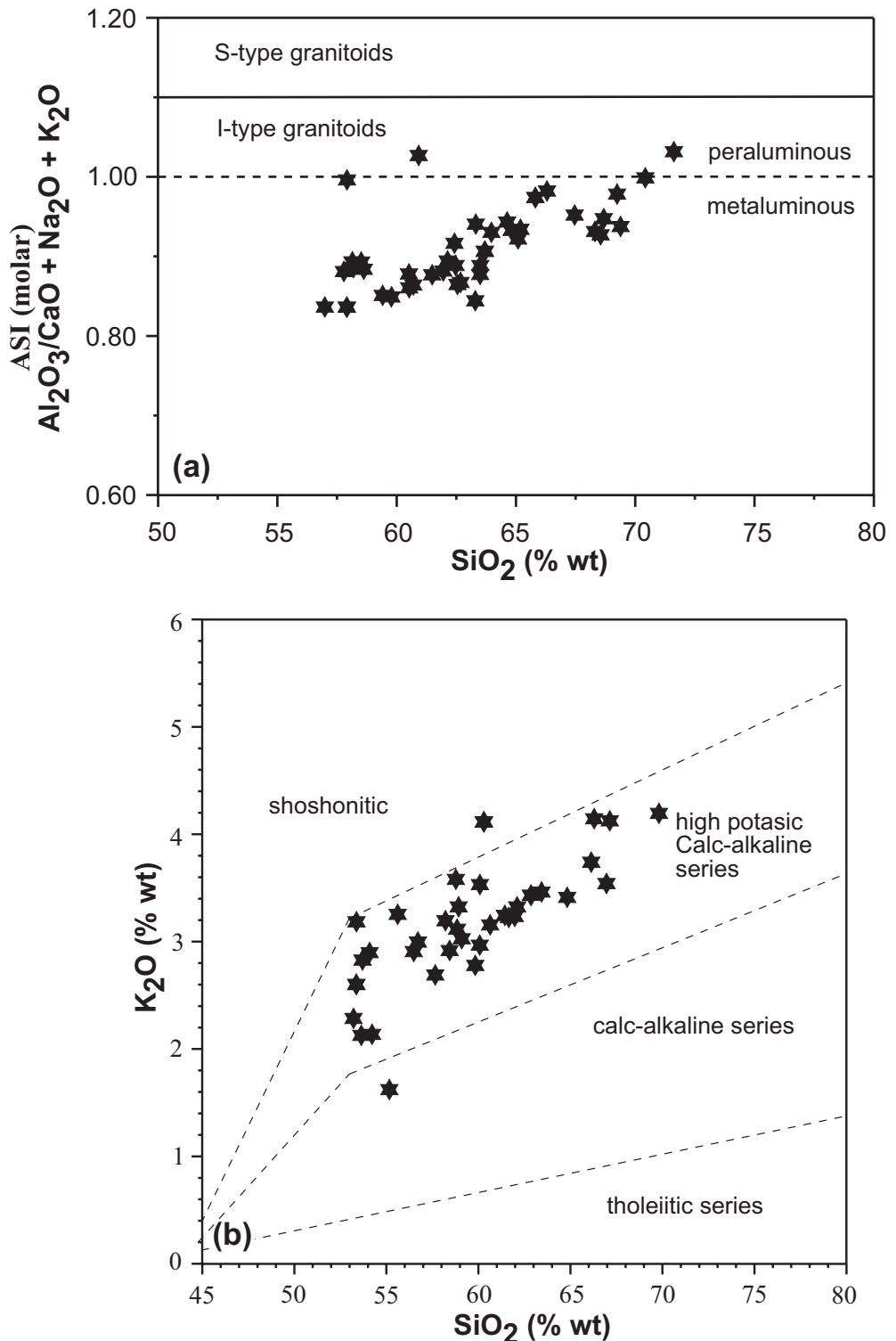


Figure 5. Aluminum saturation index [ASI = molecular $\text{Al}_2\text{O}_3/(\text{CaO}+\text{K}_2\text{O}+\text{Na}_2\text{O})$] vs SiO_2 and K_2O vs SiO_2 plots for I-type granitoid rocks from the northeastern Pontides. Tholeiitic, calc-alkaline, high-K calc-alkaline and shoshonitic field boundaries are from Peccerillo & Taylor (1976).

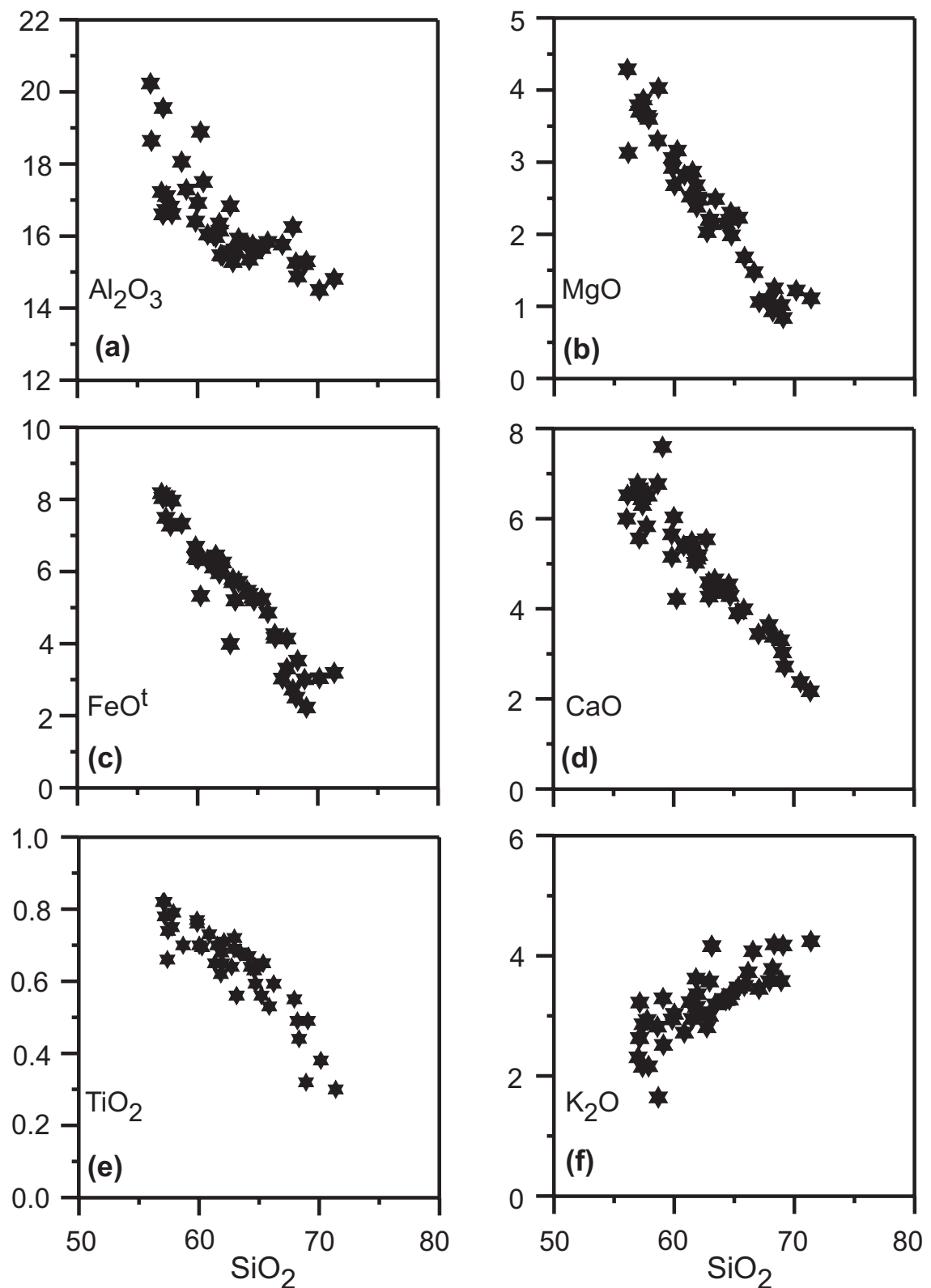


Figure 6. Selected Harker variation diagrams for I-type granitoid rocks from the northeastern Pontides.

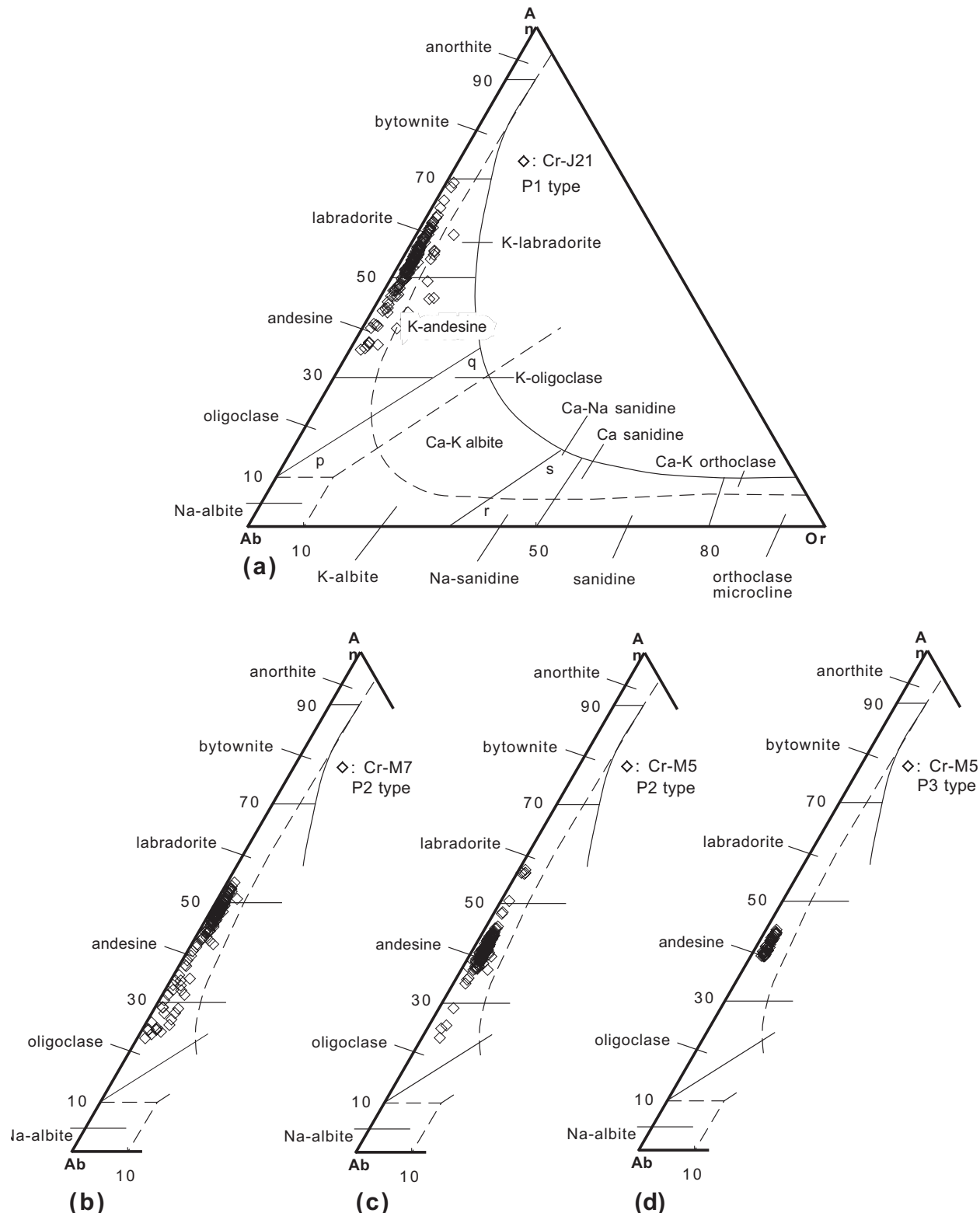


Figure 7. Compositions of zoned plagioclases and their nomenclatures. Feldspars to the right of line rs are monoclinic at all temperatures, and those above line pq are triclinic at all temperatures.

Table 2. Representative chemical compositions of the studied plagioclase crystals from the ZG.

Mineral	Plagioclase													
	P1	P1	P1	P1	P1	P1	P1	P1	P1	P2	P2	P2	P2	P2
Sample	J21-2	J21-8	J21-22	J21-48	J21-72	J21-77	J21-117	J21-139	J21-155	M7-4	M7-16	M7-21	M7-36	M7-52
SiO ₂	56.32	53.46	55.13	52.08	51.10	58.90	54.12	56.35	58.42	53.38	61.81	59.98	61.77	55.85
Al ₂ O ₃	27.37	29.72	28.54	30.42	31.20	26.17	29.44	27.14	26.34	29.34	23.33	24.42	24.25	28.31
Fe ₂ O ₃	0.29	0.39	0.18	0.42	0.43	0.21	0.49	0.41	0.27	0.28	0.15	0.29	0.31	0.34
CaO	9.03	11.70	10.47	12.67	13.56	7.56	11.38	9.12	7.43	11.09	4.34	5.19	5.25	9.97
Na ₂ O	6.31	4.86	5.53	4.25	3.72	7.17	4.93	6.13	7.21	5.32	8.96	8.70	8.54	5.90
K ₂ O	0.27	0.26	0.29	0.23	0.19	0.40	0.32	0.37	0.28	0.19	0.72	0.42	0.46	0.28
Total	99.6	100.4	100.1	100.1	100.2	100.4	100.7	99.5	99.9	99.6	99.3	99.0	100.6	100.7
Structural formula on the basis of 8 oxygens														
Si	2.541	2.412	2.482	2.364	2.321	2.624	2.432	2.545	2.613	2.425	2.765	2.700	2.731	2.500
Al	1.455	1.580	1.515	1.627	1.671	1.374	1.559	1.445	1.389	1.571	1.230	1.296	1.264	1.494
Fe ³⁺	0.010	0.013	0.006	0.014	0.015	0.007	0.017	0.014	0.009	0.010	0.005	0.010	0.010	0.011
Ca	0.437	0.566	0.505	0.616	0.660	0.361	0.548	0.442	0.356	0.540	0.208	0.250	0.248	0.478
Na	0.552	0.425	0.482	0.374	0.328	0.619	0.430	0.537	0.625	0.469	0.777	0.759	0.732	0.512
K	0.016	0.015	0.017	0.013	0.011	0.022	0.018	0.021	0.016	0.011	0.041	0.024	0.026	0.016
Total	5.011	5.011	5.007	5.008	5.006	5.007	5.004	5.003	5.008	5.026	5.026	5.039	5.011	5.011
Ab	55.0	42.2	48.0	37.3	32.8	61.8	43.2	53.7	62.7	46.0	75.7	73.4	72.7	50.9
An	43.5	56.3	50.3	61.4	66.1	36.0	55.0	44.2	35.7	52.9	40.0	24.2	24.7	47.5
Or	1.50	1.50	1.70	1.30	1.10	2.20	1.80	2.10	1.60	1.10	20.3	2.40	2.60	1.60
Sample	P2	P2	P2	P2	P2	P2	P2	P2	P2	P2	P2	P2	P2	P2
Sample	M7-89	M7-113	M7-142	M7-148	M5-2	M5-14	M5-28	M5-50	M5-119	M5-137	M5-145	M5-158	M5-168	M5-175
SiO ₂	55.55	54.53	55.18	56.55	61.75	58.74	57.22	58.12	57.58	53.89	55.32	58.60	56.11	56.96
Al ₂ O ₃	28.09	28.84	28.06	27.05	24.36	26.25	27.50	26.39	26.79	29.30	28.32	26.32	27.59	27.22
Fe ₂ O ₃	0.34	0.34	0.60	0.91	0.19	0.31	0.37	0.33	0.41	0.49	0.38	0.32	0.32	0.30
CaO	10.56	11.04	10.24	8.98	5.30	7.74	9.08	8.18	8.75	11.61	10.52	7.98	9.95	9.06
Na ₂ O	5.42	5.22	5.68	6.26	8.40	7.03	6.24	6.87	6.52	4.86	5.56	6.78	5.85	6.25
K ₂ O	0.29	0.23	0.28	0.36	0.56	0.41	0.38	0.48	0.43	0.27	0.29	0.46	0.29	0.32
Total	100.3	100.2	100.1	100.1	100.6	100.5	100.8	100.4	100.5	100.4	100.4	100.5	100.1	100.1

Table 2. continued.

Mineral	Plagioclase													
	P2	P2	P2	P2	P2	P2	P2	P2	P2	P2	P2	P2	P2	P2
Sample	M7-89	M7-113	M7-142	M7-148	M5-2	M5-14	M5-28	M5-50	M5-119	M5-137	M5-145	M5-158	M5-168	M5-175
Structural formula on the basis of 8 oxygens														
Si	2.498	2.458	2.490	2.543	2.730	2.617	2.550	2.598	2.574	2.430	2.486	2.612	2.524	2.555
Al	1.489	1.532	1.492	1.434	1.269	1.378	1.444	1.390	1.411	1.557	1.500	1.382	1.463	1.439
Fe ³⁺	0.011	0.012	0.020	0.031	0.006	0.010	0.012	0.011	0.014	0.017	0.013	0.011	0.011	0.010
Ca	0.509	0.533	0.495	0.433	0.251	0.370	0.433	0.392	0.419	0.561	0.507	0.381	0.479	0.435
Na	0.473	0.456	0.497	0.546	0.720	0.607	0.539	0.596	0.566	0.425	0.485	0.586	0.510	0.544
K	0.020	0.013	0.016	0.021	0.032	0.023	0.022	0.027	0.025	0.015	0.017	0.028	0.016	0.018
Total	5.000	5.004	5.010	5.008	5.008	5.005	5.002	5.014	5.009	5.005	5.008	5.000	5.003	5.001
Ab	47.4	45.0	49.0	55.0	71.8	60.7	54.2	58.7	56.0	42.4	48.1	59.0	50.7	54.5
An	51.0	54.0	49.0	43.0	25.0	37.0	43.6	38.6	41.5	56.0	50.3	38.4	47.7	43.7
Or	1.60	1.00	2.00	2.00	3.20	2.30	2.20	2.70	2.50	1.50	1.60	2.60	1.60	1.80
	P3	P3	P3	P3	P3	P3	P3	P3	P3	P3	P3	P3	P3	P3
Sample	M5-1-1	M5-1-2	M5-1-3	M5-1-4	M5-1-5	M5-1-6	M5-2-1	M5-2-2	M5-2-3	M5-2-4	M5-2-5	M5-2-6	M5-3-1	M5-3-4
SiO ₂	57.32	56.48	57.05	55.98	56.35	56.55	57.48	57.19	57.79	57.21	56.51	58.05	56.88	57.73
Al ₂ O ₃	27.40	27.34	27.42	27.42	27.32	27.60	27.43	27.27	27.03	26.85	26.92	26.70	26.57	26.62
Fe ₂ O ₃	0.28	0.37	0.53	0.51	0.50	0.18	0.30	0.43	0.37	0.19	0.45	0.18	0.30	0.56
CaO	9.29	9.28	9.26	9.23	9.38	9.40	8.89	8.86	8.67	8.80	8.60	8.59	8.33	8.35
Na ₂ O	6.11	6.27	6.19	6.01	6.02	6.01	6.41	6.20	6.46	6.28	6.43	6.40	6.58	6.57
K ₂ O	0.27	0.35	0.29	0.33	0.28	0.43	0.40	0.50	0.35	0.46	0.37	0.48	0.36	0.32
Total	100.7	100.1	100.7	99.5	99.9	100.2	100.9	100.5	100.7	99.8	99.3	100.4	99.0	100.2
Structural formula on the basis of 8 oxygens														
Si	2.555	2.539	2.546	2.531	2.537	2.538	2.558	2.557	2.575	2.572	2.556	2.592	2.576	2.584
Al	1.439	1.449	1.442	1.461	1.450	1.459	1.439	1.437	1.419	1.423	1.435	1.405	1.418	1.404
Fe ³⁺	0.010	0.012	0.018	0.017	0.017	0.006	0.010	0.015	0.012	0.006	0.015	0.007	0.010	0.019
Ca	0.444	0.447	0.443	0.447	0.453	0.452	0.424	0.424	0.414	0.424	0.417	0.412	0.404	0.403
Na	0.528	0.547	0.535	0.527	0.525	0.523	0.553	0.538	0.558	0.548	0.564	0.556	0.578	0.570
K	0.016	0.020	0.017	0.019	0.018	0.025	0.022	0.029	0.022	0.027	0.021	0.028	0.021	0.018
Total	4.992	5.014	5.001	5.002	5.000	5.003	50.006	5.000	5.000	5.000	5.008	5.000	5.007	4.998
Ab	53.5	54.0	54.0	53.0	52.9	52.4	55.3	54.4	56.0	58.4	56.4	55.8	58.0	57.6
An	45.0	44.1	44.4	45.0	45.5	45.2	42.5	42.8	42.0	42.6	41.5	41.5	40.0	40.6
Or	1.50	1.90	1.60	2.00	1.60	2.40	2.20	2.80	2.00	2.60	2.10	2.70	2.00	1.80

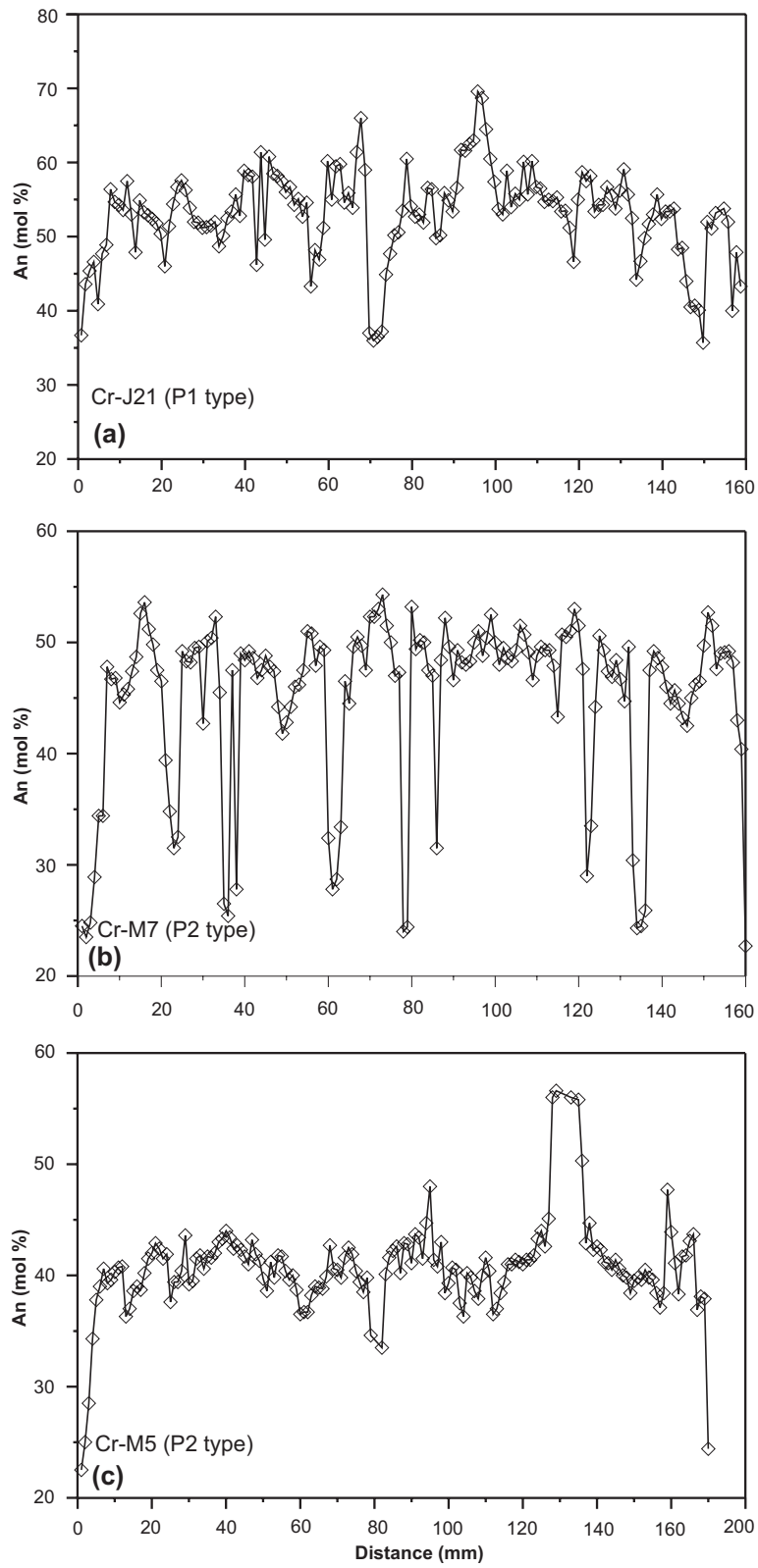


Figure 8. Electron microprobe traverses from plagioclase crystals from the ZG, pictured in Figure 4. The traverses are from the crystal to other rim.

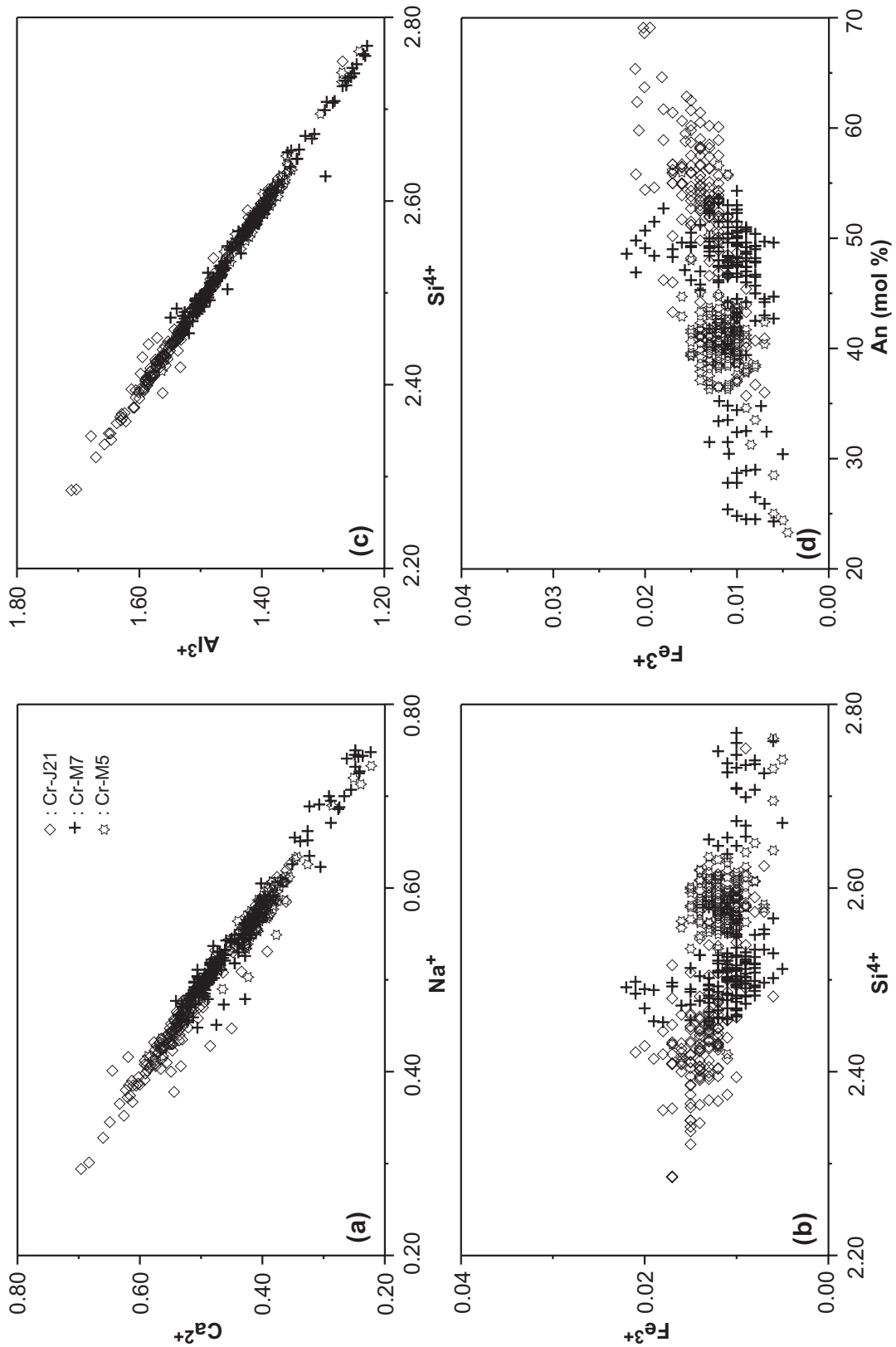


Figure 9. Plots showing mechanisms of $\text{Ca}^{2+} \leftrightarrow \text{Na}^+$, $\text{Al}^{3+} \leftrightarrow \text{Si}^{4+}$, $\text{Fe}^{3+} \leftrightarrow \text{Si}^{4+}$ substitution and Fe^{3+} versus An (mol %) content diagrams for zoned plagioclase from the ZG.

melt is a result of reaction between two compositionally different systems, i.e., felsic and mafic melts (L'Heureux & Fowler 1994). Mafic melt reacting with a felsic one is the source of mafic microgranular enclaves in the ZG. The P2-type plagioclase, more abundant in the granitic composition of the outer zone, suggests that felsic and mafic magmas interacted during crystallization of the ZG. The plagioclase morphologies and zoning patterns may result from magma interaction between a melt derived from a crustal source and mantle-derived basaltic melt. The observed zoning features and the modal mineralogical and chemical characteristics of the ZG support the supposition of a magma interaction process. This interaction model is also supported by the structure of the reversely zoned pluton (Karsli & Sadiklar 1997). In addition, An (mol %) oscillations are sharper in plagioclase of the inner zone than those in outer zone of the intrusions (Figure 8). This observation suggests that the magma interaction process may have been of greater influence in the inner zone with its monzodioritic and quartz-monzodioritic rocks than in the outer zone with its granitic and granodioritic rocks.

The plots Al^{3+} versus Si^{4+} and Ca^{2+} versus Na^+ suggest that substitution of Al^{3+} for Si^{4+} and of Ca^{2+} for Na^+ affect compositional gradients in the melt near plagioclase surfaces resulting in oscillatory zoning (Figure 9a–c). Figure 9a–c shows that the substitutions are identical in the inner and outer zones of the intrusion. This evidence suggests the thermal equilibrium occurs between felsic and mafic magmas after the interaction of two contrasting magmas.

There is a negative correlation between Fe^{3+} and Si^{4+} , possibly indicating that the substitution of Fe^{3+} for Si^{4+} be slight in plagioclase crystals of the ZG (Figure 9c). It is thought that substitution of Fe^{3+} for Al^{3+} (not shown here) may take place in plagioclase because of similarity in ionic radius between Al^{3+} and Fe^{3+} , but this substitution is less than the substitution of Fe^{3+} for Si^{4+} . Fe^{3+} concentration positively correlates with An (mol %) content (Figure 9d), and the content of Fe^{3+} increases from felsic magma to mafic magma. This correlation might be related to the reversely zoned character of the magmas that produced the ZG, because normally this content negatively correlates with An (mol %) which is a product of magma differentiation (Tegner 1997).

However, this positive correlation may also result from the stoichiometry of the plagioclase crystals.

Compiling and considering all of the data in light of the regional geology, the plutonic phases of the northeastern Pontides crystallized as a consequence of north-dipping subduction beneath the Eurasian plate. Moreover, textural and geochemical evidence suggest that contrasting coeval mafic (mantle-derived) and felsic (crustal-derived) magmas may have contributed to the evolution of arc magmatism in the eastern Pontides.

Conclusions

The zoned compositions of plagioclase in the ZG clearly contain valuable information concerning the magmatic history of the pluton. A number of petrogenetically significant textural and chemical characteristics of the zoned plagioclase suggest the following results:

1. The plagioclase crystals in the Zigana Granitoid display oscillatory zoning with spongy-cellular cores, possibly caused by magma interaction via mafic magma injection into the felsic magma chamber of the intrusion.
2. The zoned plagioclase compositions, governed by strong substitution of $\text{Al}^{3+} \leftrightarrow \text{Si}^{4+}$, $\text{Ca}^{2+} \leftrightarrow \text{Na}^+$, and slight substitution of $\text{Fe}^{3+} \leftrightarrow \text{Si}^{4+}$, indicates that thermal equilibrium developed between felsic and mafic magmas during crystallization.
3. Magma interaction via recurrent mafic magma injection into a felsic magma chamber was an operative magmatic process during crystallization of the pluton.
4. The ZG formed by fractional crystallization as revealed by this detailed investigation of plagioclase zonation.
5. The ZG is part of a plutonic phase, described as arc magmatism of Albian to Oligocene age, which developed by northward subduction beneath the Eurasian continental margin. We suggest that fractional crystallization and magma interaction, which played important roles in the evolution of the ZG, may also have been influential processes in the evolution of other granitoids of the Pontide Belt insofar as the ZG is representative of all granitoids in the belt.

Acknowledgements

The authors thank Rainer Altherr for providing microprobe analyses and helpful discussions, Hans Peter Meyer for supplying mineral calculation software and Ilona Fin for preparing the polished sections in the Mineralogical Institute of Heidelberg University,

Germany. The first author acknowledges the financial support of DAAD through a scholarship program. The authors are grateful to Cüneyt Şen of Karadeniz Technical University for his encouragement and suggestions. Erdin Bozkurt and two anonymous reviewers provided helpful comments on an earlier draft of the manuscript.

References

- ANDERSON, A.L., JR. 1984. Probable relations between plagioclase zoning and magma dynamics, Fuego Volcano, Guatemala. *American Mineralogist* **69**, 660–676.
- BEKTAŞ, O. 1986. Paleostress trajectories and polyphase rifting in the arc, back-arc of the eastern Pontides. *General Directorate of Mineral Research and Exploration of Turkey (MTA) Bulletin* **103/104**, 1–15.
- BEKTAŞ, O., YILMAZ, C., TASLI, K., AKDAĞ, K. & ÖZGÜR, S. 1995. Cretaceous rifting of the Eastern Pontide Carbonate Platform, NE Turkey: the formation of carbonate breccias and turbidites as evidence of a drowned platform. *Geologie* **57**, 233–244.
- BEKTAŞ, O., ŞEN, C., ATICI, Y. & KÖPRÜBAŞI, N. 1999. Migration of the Upper Cretaceous subduction-related volcanism towards the back-arc basin of the Eastern Pontide magmatic arc (NE Turkey). *Geological Journal* **34**, 95–106.
- BOZTUĞ, D. 2001. *Suçehri (Sivas) – Gölköy (Ordu) Arasında KAFZ'nun Kuzey ve Güney Kesimlerindeki Granotoidlerin ve Çevre Kayaçlarının Petrolojik İncelenmesi* [Petrography of Granitoids and Country Rocks to the North and South of the North Anatolian Fault Zone in the Area Between Suçehri (Sivas) and Gölköy (Ordu)]. TÜBİTAK Project Report, No: 195Y001, 113 p [in Turkish with English abstract, unpublished].
- BOZTUĞ, D., ERÇİN, A.İ., GÖÇ, D., ER, M., İSKENDERÖĞLU, A., KURUÇELİK, M.K. & KÖMÜR, İ. 2001. Petrogenesis of the composite Kaçkar Batholith along a north–south geotraverse between Ardeşen (Rize) and İspir (Erzurum) towns, eastern Black Sea. *Fourth International Turkish Geology Symposium, Abstracts*, 24–28 September, Adana, p. 210.
- BOZTUĞ, D., JONCKHEERE, R., WAGNER, G.A. & YEĞİNGİL, Z. 2004a. Slow Senonian and fast Paleocene–Early Eocene uplift of the granitoids in the central eastern Pontides, Turkey: apatite fission-track results. *Tectonophysics* **382**, 213–228.
- BOZTUĞ, D., ERÇİN, A.İ., KURUÇELİK, M.K., Göç, D., KÖMÜR, İ. & İSKENDERÖĞLU, A. 2004b. Main geochemical characteristics of the composite Kaçkar batholith derived from the subduction through collision to extensional stages of the Neo-Tethyan convergence system in the Eastern Pontides, Turkey. *Journal of Asian Earth Sciences*, in press.
- CASTRO, A. 2001. Plagioclase morphologies in assimilation experiments: implications for disequilibrium melting in the generation of granodiorite rocks. *Mineralogy and Petrology* **71**, 31–49.
- ÇOCAULLU, H.E. 1975. *Gümüşhane ve Rize Yörelerinde Petrolojik ve Jeokronolojik Araştırmalar* [Petrographic and Geochronologic Study in the Gümüşhane and Rize Regions]. İstanbul Technical University Publications **1034**, 112 p.
- GEDİK, A., ERCAN, T., KORKMAZ, S. & KARATAŞ, S. 1992. Rize-Fındıklı-Çamlıhemşin arasında (Doğu Karadeniz) yer alan magmatik kayaçların petrolojisi ve Doğu Pontidlerdeki bölgesel yayılımları [Petrology of magmatic rocks in the Rize-Fındıklı-Çamlıhemşin (east Black Sea) area and their distribution in the eastern Pontides]. *Geological Bulletin of Turkey* **35**, 15–38 [in Turkish with English abstract].
- GÜVEN, İ.H. 1993. *Doğu Pontidler'in 1/250,000 Ölçekli Kompilasyonu* [1/250,000 Scale Compilation of the Eastern Pontides]. General Directorate of the Mineral Research and Exploration Institute of Turkey (MTA) Report No: 90944 [unpublished, in Turkish].
- HATTORI, K. & SATO, H. 1996. Magma evolution recorded in plagioclase zoning in 1991 Pinatubo eruption products. *American Mineralogist* **81**, 982–994.
- HIBBARD, M.J. 1991. Textural anatomy of twelve magma-mixed granitoid systems. In: DIDIER, J. & BARBARIN, B. (eds), *Enclaves and Granite Petrology* **13**, 431–444.
- HOUSH, T.B. & LUHR, J.F. 1991. Plagioclase–melt equilibria in hydrous systems. *American Mineralogist* **76**, 477–492.
- JICA, 1986. *The Republic of Turkey Report on the Cooperative Mineral Exploration of Gümüşhane Area*. Consolidated report. Japan International Cooperation Agency, Metal Mining Agency of Japan [unpublished report].
- JOHANNES, W. 1978. Melting of plagioclase in the system Ab-An-H₂O and Qz-Ab-An-H₂O at fH₂O = 5 kbars, an equilibrium problem. *Contributions to Mineralogy and Petrology* **66**, 295–303.
- KANDEMİR, R. & KORKMAZ, S. 1999. Depositional system in the eastern Pontides back-arc basin: an example from South of Artvin, NE-Turkey. *Zentralblatt für Geologie und Paläontologie* **10–12**, 1495–1504.
- KARSLI, O. 1996. *Zigana Granitoidinin (Maçka-Trabzon) Mineralojik ve Jenetik Açıdan İncelenmesi* [Mineralogy and Genesis of the Zigana Granitoid (Maçka-Trabzon)]. MSc Thesis, Karadeniz Technical University, Trabzon [in Turkish with English abstract, unpublished].

- KARSLI, O. 2002. *Granitoid Kayaçlarda Magma Etkileşimleri İçin Petrografik, Mineralojik ve Kimyasal Bulgular: Dölek ve Sarçık Plütonları (Gümüşhane, KD-Türkiye)* [Petrographic, Mineralogic and Chemical Evidence for Magma Interaction in Granitoid Rocks: Dölek and Sarçık Plutons (Gümüşhane, NE-Turkey)]. PhD Thesis, Karadeniz Technical University, Trabzon, [in Turkish with English abstract, unpublished].
- KARSLI, O. & SADIKLAR, M.B. 1996. Mineralogy and genesis of Zigana Granitoid (NE-Turkey). *Beihefte zum European Journal of Mineralogy* 8, 133 p.
- KARSLI, O. & SADIKLAR, M.B. 1997. Granitoid kayaçların mineralojik değişiminin belirlenmesinde yeni bir yaklaşım: Zigana Granitoidi (Maçka-Trabzon) [A new approach to identifying mineralogic changes in granitoid rocks: Zigana Granitoid (Maçka-Trabzon)]. *Geosound (Yerbilimleri)* 30, 601–612 [in Turkish with English abstract]
- KARSLI, O., AYDIN, F. & SADIKLAR, M.B. 2002. Geothermobarometric investigation of the Zigana Granitoid, eastern Pontides, Turkey. *International Geology Review* 44, 277–286.
- KARSLI, O., AYDIN, F. & SADIKLAR, M.B. 2004a. The morphology and chemistry of K-feldspar megacrysts from İkizdere Pluton: evidence for acid and basic magma interactions in granitoid rocks, NE-Turkey. *Chemie der Erde - Geochemistry* 64, 155–170.
- KARSLI, O., AYDIN, F., SADIKLAR, M.B., ALTHERR, R. & UYSAL, İ. 2004b. Higher degrees hybridisation in Eocene aged granitoidic rocks, NE-Turkey: as indicator of oxygen fugacity from mafic microgranular enclaves and host rocks. *5th International Symposium on Eastern Mediterranean Geology, Abstracts*, 14–20 April, Thessaloniki, 1147–1150.
- KESKİN, İ., KORKMAZ, S., GEDİK, İ., ATEŞ, M., GÖK, L., KÜCÜMEN, O. & ERKAL, T. 1989. Geology of the region around Bayburt. *General Directorate of the Mineral Research and Exploration Institute of Turkey (MTA)* Report No: 8995, 128 p.
- KETİN, İ. 1966. Turkiyenin tektonik birlükleri [Tectonic units of Turkey]. *General Directorate of the Mineral Research and Exploration Institute of Turkey (MTA) Bulletin* 66, 23–24.
- KUŞCU-GENÇALIOĞLU, G. & FLOYD, P.A. 2001. Mineral compositional and textural evidence for magma mingling in the Saraykent volcanics. *Lithos* 56, 207–230.
- L'HEUREUX, I. & FOWLER, A.D. 1994. A nonlinear dynamical model of oscillatory zoning in plagioclase. *American Mineralogist* 79, 885–891.
- LOFGREN, G.E. & DONALDSON, C.H. 1975. Curved branching crystals and differentiation in comb-layered rocks. *Contributions to Mineralogy and Petrology* 49, 309–319.
- LUHR, J.F. & MELSON, W.G. 1996. Mineral and composition in June 15 1991, pumices: evidence for dynamic disequilibrium in the Pinatubo dacite. In: PUNOBAYAN, R.S & NEWHALL, C.G. (eds), *Fire and Mud Eruptions and Lahars of Mount Pinatubo, Philippines*, 733–750.
- MCDOWELL, S.D. 1978. Little Chief granite porphyry: feldspar crystallization history. *Geological Society of America Bulletin* 89, 33–49.
- MOORE, W.J., MCKEE, E.H. & AKINCI, Ö. 1980. Chemistry and chronology of plutonic rocks, in the Pontide mountains, Northern Turkey. *European Cooper Deposits, Belgrade*, 209–216.
- NELSON, S.T. & MONTANA, A. 1992. Sieve-textured plagioclase in volcanic rocks produced by rapid decompression. *American Mineralogist* 77, 1242–1249.
- OKAY, A.İ. 1993. *Geology and Tectonic Evolution of the Pulur (Bayburt) Region*. Turkish Petroleum Exploration Division (TPAO) Report No: 3415, 86 p.
- OKAY, A.İ. 1996. Granulite facies gneisses from the Pulur region, eastern Pontides. *Turkish Journal of Earth Sciences* 5, 55–61.
- OKAY, A.İ. & ŞAHİNTÜRK, O. 1997. Geology of the eastern Pontides. In: ROBINSON, A.G. (ed), *Regional and Petroleum Geology of the Black Sea and Surrounding Region*. American Association of Petroleum Geologist Memoir 68, 291–310.
- PECCERILLO, A. & TAYLOR, S.R. 1976. Geochemistry of Eocene calc-alkaline volcanic rocks from the Kastamonu area, northern Turkey. *Contributions to Mineralogy and Petrology* 58, 63–81.
- PRINGLE, G.J., TREMBATH, L.T. & PAJARI, G.E. 1974. Crystallization history of a zoned plagioclase. *Mineralogical Magazine* 39, 867–877.
- ŞENGÖR, A.M.C. & YILMAZ, Y. 1981. Tethyan evolution of Turkey: a plate tectonic approach. *Tectonophysics* 75, 181–241.
- ŞENGÖR, A.M.C., ÖZEREN, S., GENÇ, T & ZOR, E. 2003. East Anatolian high plateau as a mantle-supported, north-south shortened domal structure. *Geophysical Research Letters* 30(24), 8044, doi: 10.1029/2003GL018192.
- STOMER, J.C. 1972. Mineralogy and Petrology of the Raton-Clayton volcanic field, northeastern New Mexico. *Geological Society of America Bulletin* 83, 3299–3322.
- TANER, M. F. 1977. *Etude géologique et Petrographique de la Région de Gümüşhane, İkizdere, Située au sud de Rize (Pontides Orientales, Turquie)*. PhD Thesis, University of Geneve, Geneve [unpublished].
- TEGNER, C. 1997. Iron in plagioclase as a monitor of the differentiation of the Skaergaard intrusion. *Contributions to Mineralogy and Petrology* 128, 45–51.
- TSUCHIYAMA, A. 1985. Dissolution kinetics of plagioclase in melt of the system diopside-albite-anorthite and the origin of dusty plagioclase in andesites. *Contributions to Mineralogy and Petrology* 89, 1–16.
- YODER, H.S., STEWART, D.B., & SMITH, J.R. 1957. Ternary feldspar. *Carnegie Institution of Washington Year Book* 56, 206–214.
- YILMAZ, C. 1995. Gümüşhane-Bayburt yöresindeki Alt Jura çökellerinin fasiyesi ve ortamsal nitelikleri (KD Türkiye) [Facies and environmental characteristics of Lower Jurassic sediments in Gümüşhane-Bayburt region]. *Geosound (Yerbilimleri)* 26, 119–128 [in Turkish with English abstract].

- YILMAZ, C. 1996. Doğu Pontid Karbonat Platformu'nun kırılmasına ilişkin yeni bulgular [Evidence about the break-up of eastern Pontide carbonate platform]. *2nd Turkish Petroleum Congress Proceedings*, 190–198 [in Turkish with English abstract].
- YILMAZ, C. 1997. The sedimentological records of the platform basin transition in the Gümüşhane Region NE Turkey. *Geology Mediterranean* **24**, 125–135.
- YILMAZ, C. 2002. Gümüşhane-Bayburt Yöresindeki Mesozoyik havzalarının tektono-sedimentolojik kayıtları ve kontrol etkenleri [Tectono-sedimentary records and controlling factors of Mesozoic basins in Gümüşhane-Bayburt region]. *Geological Bulletin of Turkey* **45**, 141–164 [in Turkish with English abstract].
- YILMAZ, C. & KARSLI, O. 1997. Maçka-Zigana yöresinde Üst Kretase sürecindeki çökel kayıtları ve bölge jeolojisindeki önemi [Late Cretaceous sedimentary record in Maçka-Zigana region and its geologic significance]. *Geosound (Yerbilimleri)* **30**, 331–340 [in Turkish with English abstract].
- YILMAZ, S. & BOZTUĞ, D. 1996. Space and time relations of three plutonic phases in the eastern Pontides, Turkey. *International Geology Review* **38**, 935–956.
- YILMAZ, Y., TÜYSÜZ, O., YİĞİTBAŞ, E., GENÇ, Ş.C. & ŞENGÖR, A.M.C. 1997. Geology and Tectonic Evolution of the Pontides. In: ROBINSON, A.G. (ed), *Regional and Petroleum Geology of the Black Sea and Surrounding Region*. American Association of Petroleum Geologists Memoir **68**, 183–226.
- VANCE, J.A. 1962. Zoning in igneous plagioclase: normal and oscillatory zoning. *American Journal of Science* **260**, 746–760.
- VANCE, J.A. 1965. Zoning in igneous plagioclase: patchy zoning. *Journal of Geology* **73**, 637–651.
- WIEBE, R.A. 1968. Plagioclase stratigraphy: a record of magmatic conditions and events in a granite stock. *American Journal of Science* **266**, 670–703.

Received 10 October 2003; revised typescript accepted 20 August 2004